

Catalysts for single-wall carbon nanotube synthesis—From surface growth to bulk preparation

Xiulan Zhao,* Shuchen Zhang,* Zhenxing Zhu,* Jin Zhang, Fei Wei, and Yan Li

Catalysts play essential roles in the chemical vapor deposition of single-wall carbon nanotubes (SWCNTs). In this article, we summarize studies on catalysts for the structure-controlled growth and mass production of SWCNTs, discussing the main progress and the remaining challenges.

Introduction

Single-wall carbon nanotubes (SWCNTs) are one of the most distinctive cylindrical one-dimensional nanomaterials that have stimulated extensive research in multidisciplinary fields.¹ Besides the state-of-the-art investigations on the preparation and properties of SWCNTs in laboratories, efforts in mass production are ongoing and scalable products involving energy storage and composites are commercially available.²

Compared with arc discharge and laser ablation synthesis methods, catalytic chemical vapor deposition (CCVD) has advantages of higher capacity and simpler equipment, and has become the most prevalent method for the bulk synthesis of SWCNTs. Several manufacturers have transformed the technology from universities to produce SWCNTs in bulk with the production capacity of approximately 1.0–1.5 ton per age (t/a).³

Because many electronic and optoelectronic properties are due to the chiral structure of SWCNTs,⁴ which is denoted by indices (n, m) , chirality control is critical for higher-end applications ranging from electronics to biomedicine. Because of their good dispersion and discrete morphology, surface-grown SWCNTs provide a better platform for studying the growth mechanism and ways of controlling the synthesis. Some recent major breakthroughs have been made using surface-grown

SWCNTs involving the control of chirality,^{5–7} density,⁸ length,^{9,10} and conductive properties.¹¹

Catalysts play vital roles in the structure control of SWCNTs in both surface and bulk synthesis. Thermodynamically, the chirality of a SWCNT becomes locked in when the final (sixth) pentagon is added to the hemisphere during nucleation,¹² revealing an essential matching of symmetry between SWCNTs and the crystal surface of the catalyst particles.^{6,7} Kinetically, precise control of the growth conditions is crucial for prolonging the lifetime of catalyst nanoparticles in order to grow perfect, ultralong CNTs with a uniform structure.⁹

The relationships between catalyst design and dispersion methods and corresponding growth mechanism are still not clear. Especially, differences between the thermodynamic characteristics and phase diagrams of the bulk catalyst and its nanoparticles, as used in SWCNT production, make mass production more complicated. The size, composition, dispersion state, and interaction with supporting materials can directly affect thermal transport, surface/bulk diffusion, and the quality of the as-grown SWCNTs. In this article, we review progress in catalyst synthesis and dispersion methods for SWCNT growth and elaborate on recent strategies for the controlled synthesis of surface and bulk SWCNTs by tailoring these catalysts.

*These authors contributed equally to the article.

Xiulan Zhao, Peking University, China; xiulanzhls@pku.edu.cn

Shuchen Zhang, Peking University, China; zhangsc-cnc@pku.edu.cn

Zhenxing Zhu, Tsinghua University, China; zzx15@mails.tsinghua.edu.cn

Jin Zhang, Peking University, China; jinzhang@pku.edu.cn

Fei Wei, Tsinghua University, China; wf-dce@mail.tsinghua.edu.cn

Yan Li, Peking University, China; yanli@pku.edu.cn

doi:10.1557/mrs.2017.240

Catalyst design for diameter-controlled growth of SWCNTs

Diameter is one important parameter influencing the electronic properties of SWCNTs.¹³ Precise control of the diameter is a primary factor for stopping the formation of metallic SWCNTs and achieving preferential growth of semiconducting SWCNTs,¹⁴ both of which are essential for field-effect transistors (FETs). Therefore, the selective growth of SWCNTs with a controlled diameter, especially with an extremely narrow distribution, is important. The catalyst plays the most important role in the CVD process in determining the SWCNT diameter compared with other factors, such as temperature¹⁵ and carbon feedstock.¹⁶ The size of the catalyst nanoparticles always has a positive correlation with the SWCNT diameter,^{17–20} as shown in **Figure 1a**. Therefore, methods for controlling the catalyst particle size and its stabilization during the CVD process are necessary for controlling the diameter of SWCNTs in large-scale production.

Catalyst nanoparticles are usually obtained by reducing the corresponding precursors, so the morphology and dispersion of the precursor seriously affects the catalyst size and are important factors.

General methods to control the diameter of SWCNTs

At the early stage of controlling the SWCNT diameter, many methods have been developed to prepare homogeneous and monodispersed precursors to obtain uniform nanoparticles of the metal catalyst, such as Fe and Ni-Fe. There are three main strategies: (1) capping agent-protected synthesis of nanoparticles; (2) using special cages to trap a fixed number of metal ions to act as the catalyst precursor; and (3) using polyoxo-metalate (POM) nanoclusters with an identical structure as the catalyst precursor.

Capping agents attach to the surface of metal nanoparticles by coordination or static charge interactions, thus tuning the growth behavior of SWCNTs and eventually resulting in nanoparticles with a very small size and a narrow size distribution. Liu et al. obtained Fe–Mo catalysts with a size deviation as small as ~7–8% by using a mixture of carboxylic acid and amine as the capping agent (Figure 1b) where increasing the amount of carboxylic acid increased the catalyst particle size.²¹ Similarly, Lieber's group realized diameter control of SWCNTs by changing the chain length of capping agents.¹⁸ Other work involved using iron-storage protein, ferritin, to trap a certain number of metal ions. Dai et al. synthesized discrete catalyst particles with a tunable diameter by changing the amount of iron in ferritin, as shown in Figure 1c.²²

A family of polyatomic oxyanions of transition metals (POMs [such as Mo, W, V, Nb, and Ta])²³ are assembled with many metallic oxide polyhedra linked to each other by sharing corners and edges and therefore have definite sizes and shapes with discrete cluster structures. W and Mo are metals with high melting points, and POMs are convenient precursors for W- or Mo-containing catalysts, such as nanoparticles of monometallic Mo, bimetallic Fe–Mo, Fe–W, and W–Co.²³ Usually this method leads to a narrower particle-size distribution of the catalyst than other methods. However, for the preparation of catalysts containing Mo, correct annealing and reducing conditions are necessary because MoO₃ is easily vaporized at temperatures above 600°C, and this is unfavorable for obtaining a uniform catalyst particle size.^{24,25} Zhang et al. used Mo catalysts prepared at a low reducing temperature and obtained semiconducting SWCNTs with a narrow diameter distribution on a quartz substrate (**Figure 2a**).²⁵ Compared with a Mo-containing cluster, W-containing nanocatalysts, shown in Figure 2b, may be a better choice since WO₃ is more stable.^{7,26,27} Undoubtedly, catalysts with a high melting point and specific size have proven to be helpful in controlling the diameter of SWCNTs.

When a dispersion solution of catalyst nanoparticles is dropped on a substrate, they

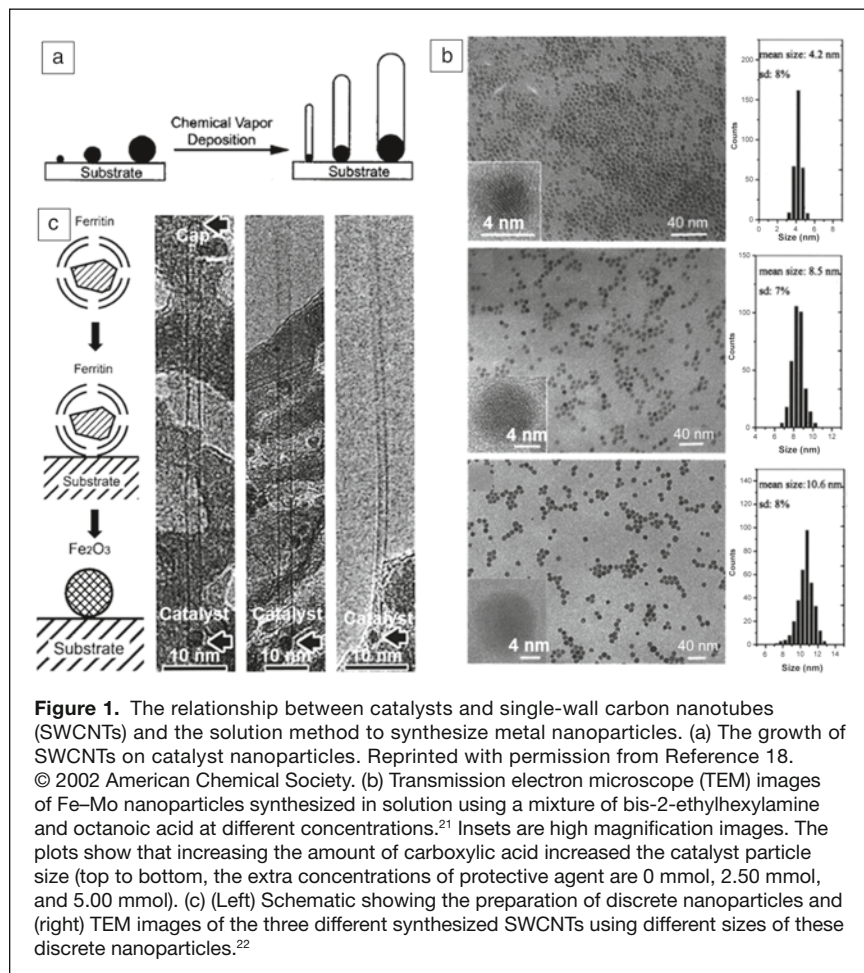
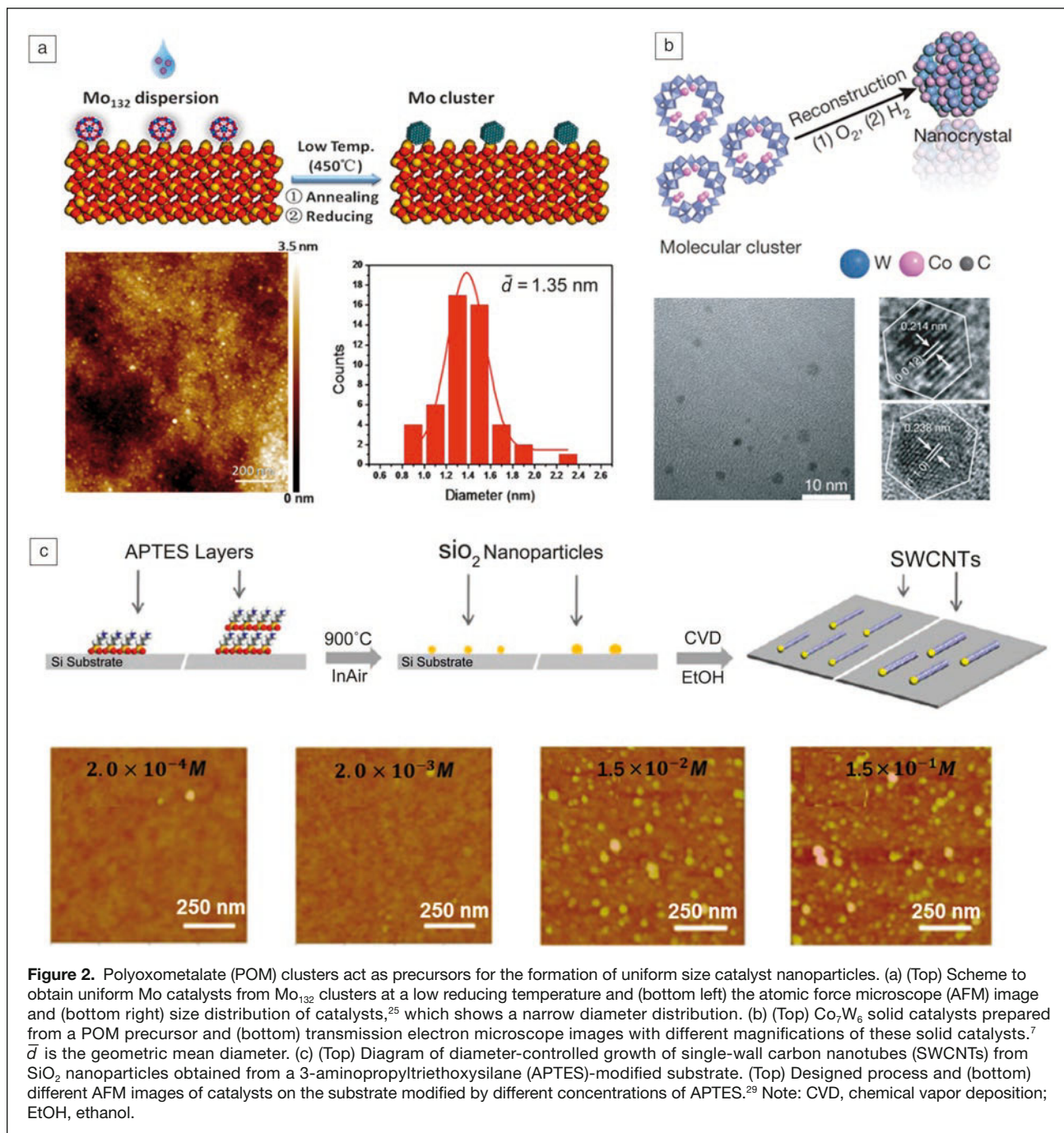


Figure 1. The relationship between catalysts and single-wall carbon nanotubes (SWCNTs) and the solution method to synthesize metal nanoparticles. (a) The growth of SWCNTs on catalyst nanoparticles. Reprinted with permission from Reference 18. © 2002 American Chemical Society. (b) Transmission electron microscope (TEM) images of Fe–Mo nanoparticles synthesized in solution using a mixture of bis-2-ethylhexylamine and octanoic acid at different concentrations.²¹ Insets are high magnification images. The plots show that increasing the amount of carboxylic acid increased the catalyst particle size (top to bottom, the extra concentrations of protective agent are 0 mmol, 2.50 mmol, and 5.00 mmol). (c) (Left) Schematic showing the preparation of discrete nanoparticles and (right) TEM images of the three different synthesized SWCNTs using different sizes of these discrete nanoparticles.²²



tend to aggregate and form random agglomerates, which does not help produce uniform catalyst nanoparticles. Liu et al. modified a silicon dioxide surface using 3-aminopropyltriethoxysilane (APTES).²⁸ The modified surface terminated by amine groups becomes positively charged, such that negatively charged species assemble on the surface through Coulombic attraction. Alkyl amine and alkyl carboxylic acid capped Fe–Mo nanoparticles can be uniformly distributed on these substrates.²⁸ Coincidentally, Zhang’s group directly grew SWCNTs on a silicon dioxide surface that had been modified by APTES and found that the diameter distribution of the nanotubes correlated with that of the

SiO_2 nanoparticles (Figure 2c).²⁹ The size of the SiO_2 nanoparticles was increased by increasing the number of APTES layers deposited on the silicon dioxide surface, thus producing a larger SWCNT diameter.

Specific methods for controlling the diameter of SWCNTs in a horizontal array

On a flat substrate there are two main processes that affect the size distribution of catalyst nanoparticles, aggregation occurring in the calcination and reduction processes and Ostwald ripening in the reduction and CVD processes. In Ostwald

ripening, larger nanoparticles grow at the expense of small nanoparticles. These two effects make it difficult to obtain a SWCNT horizontal array with a narrow diameter distribution because they lead to nanoparticles with a broader size distribution, which is unfavorable for the growth of SWCNTs with a uniform diameter. However, strong interaction between the catalyst nanoparticles and the substrate will help retain the narrow size distribution of the catalytic nanoparticles. To strengthen this interaction, thermal annealing is used.

Ago et al. found that thermal annealing in an ultrahigh vacuum followed by H_2 reduction for 1 h resulted in catalyst nanoparticles with a narrow size distribution.³⁰ Using these catalysts, horizontally aligned SWCNTs with a very narrow diameter distribution, 76% of which have diameters between 1.3 and 1.4 nm, were obtained. Zhang et al. designed a special annealing process at a temperature of $\sim 1100^\circ\text{C}$ that buries Fe_2O_3 in the sapphire substrate⁸ to reduce catalyst aggregation. Since Fe_2O_3 has a similar crystal structure to sapphire, Al^{3+} can be partially replaced by Fe^{3+} in the sapphire substrate due to the entropy effect. As shown in **Figure 3a**,⁸ by introducing hydrogen, Fe^{3+} ions were reduced and released from the substrate, forming the active catalyst to grow SWCNTs. Because of the strong interaction between the freshly formed catalyst particles and the sapphire substrate, aggregation was avoided, and a horizontal SWCNT array with an ultrahigh density of ~ 130 tubes/ μm was obtained. Zhang's group modified this process⁶ to improve the uniformity of the particles. As shown in **Figure 3b**,⁶ monodispersed MoO_3 formed on sapphire through an annealing process. Using a lower reducing temperature, they slowed the reducing rate and thus produced Mo_2C catalyst particles of uniform size, with nearly 90% of the particles having diameters between 1.1 nm and 1.5 nm. Since Mo_2C has a high melting point and,

therefore, a lower vapor pressure, aggregation and Ostwald ripening were largely suppressed. This method was also used to prepare uniform solid WC catalysts with a small size. These uniform carbide catalysts were used to synthesize $(2n, n)$ type SWCNTs.⁶

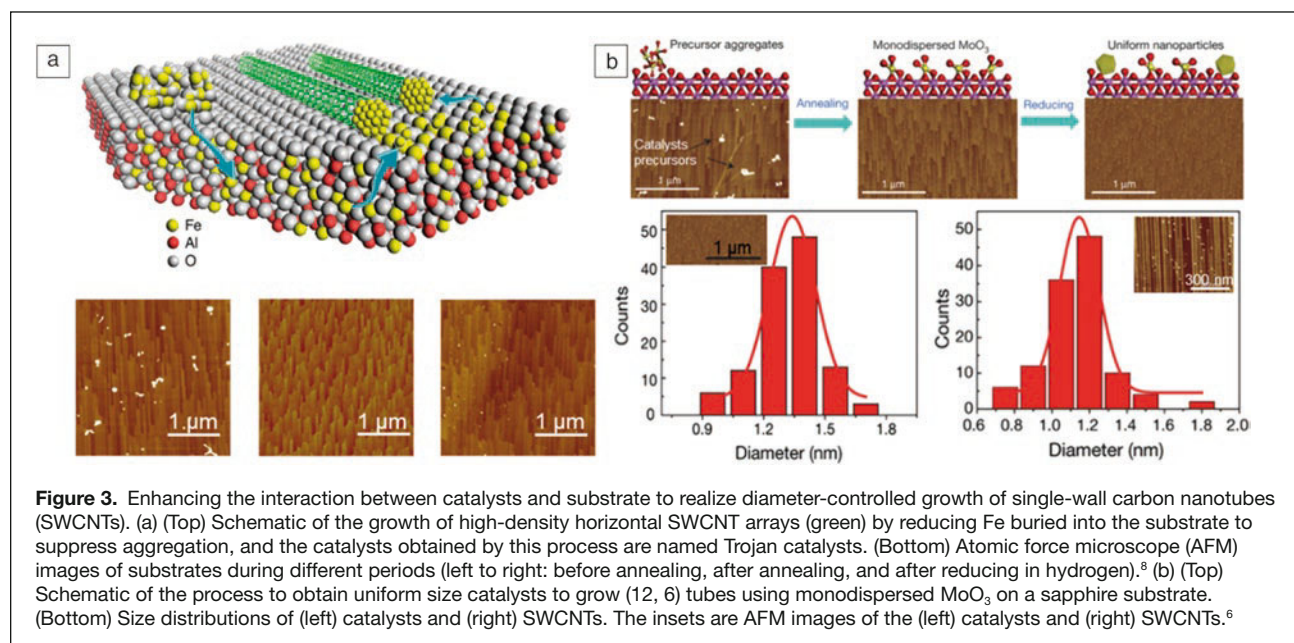
In summary, the diameter of the SWCNTs highly depends on the size of the catalyst particles. To achieve diameter-controlled growth of SWCNTs by CVD, a rational choice and design of the catalyst as well as the supporting substrates is necessary to maintain uniform size of the catalyst nanoparticles.

Chirality-controlled growth of SWCNTs

Chirality-specific SWCNTs have shown outstanding performance in many applications such as high-resolution multicolor biological imaging,³¹ high-efficiency photovoltaic processes,^{32,33} and photocatalytic water splitting.³⁴ To prepare chirality-specific SWCNTs, researchers have made significant efforts in the past two decades.^{35,36} The formation process of a SWCNT has been observed with TEM and has shown that carbon caps first nucleate on the catalyst, then grow into well-defined tubes by the addition of more carbon atoms.¹⁷ Therefore, the SWCNT chirality is directly related to the structure of the carbon cap and can even be determined by the structure of the cap with a suitable and stable carbon supply.

Chirality-controlled growth of SWCNTs by catalysts supported on flat substrates

There are two approaches to achieve chirality selective growth of SWCNTs. One is epitaxial growth SWCNT from well-defined SWCNT segments, such as segments of SWCNTs with specific chirality and caps from opening fullerenes or cyclodehydrogenation of polycyclic hydrocarbon precursors.



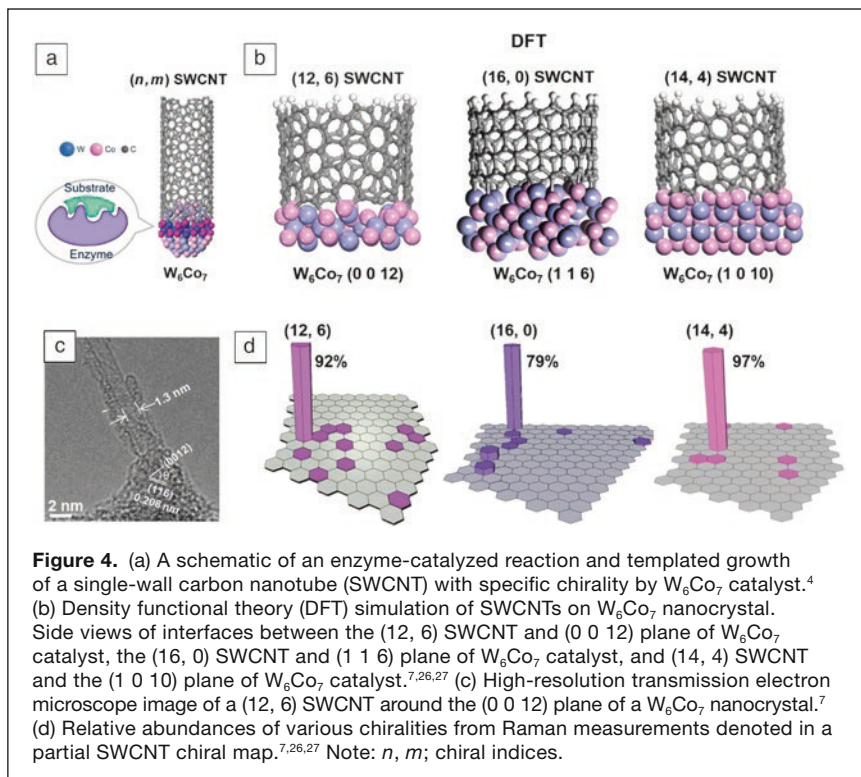
The Smalley group used SWCNTs with metal nanoparticles docked on the open ends as the catalysts to restart the SWCNT growth.³⁷ The produced SWCNTs thus had the same chirality as the seed tubes. Ultrashort capped (6, 6) nanotubes were synthesized by Pt-catalyzed cyclodehydrogenation of the well-designed polycyclic hydrocarbon precursor $C_{96}H_{54}$.⁵ The resultant ultrashort capped (6, 6) nanotubes were elongated into long SWCNTs with the same chirality through the incorporation of more carbon atoms. The use of SWCNT seeds to achieve chirality-controlled growth of SWCNTs has made great progress, but increasing the stability of the seeds and the yield and efficiency of SWCNT production remains a challenge.

The second method is to control the structure of the SWCNT cap through catalyst-epitaxial growth, since theoretical simulation has demonstrated that lattice-matched caps are more stable.³⁸ Fouquet et al. realized the dominant growth of (6, 5) SWCNTs with an abundance of 27% from a Co catalyst on an oxidized Si wafer.³⁹ The selectivity was attributed to the homogeneous Co catalyst nanoparticles stabilized by interfacial Co–Si interactions. Preferential growth of (16, 2) tubes was achieved using Co–Mo catalysts on the (1 1 -2 0) plane of sapphire, while SWCNTs grown on the (1 -1 0 2) plane are dominated by the near-armchair SWCNTs.⁴⁰ They speculated that the different atomic structures of the (1 1 -2 0) and (1 -1 0 2) plane sapphire surfaces induced different morphologies and orientations of the catalysts, which then influenced the SWCNT chirality. Great efforts have been devoted to improve the chiral selectivity of the SWCNTs through regulating the catalyst size, composition, and morphology. Nevertheless, chiral selectivity of SWCNTs is still far from satisfactory.

Li et al., inspired by the extremely high selectivity of enzyme-catalyzed reactions endowed by the molecular recognition effect, proposed that a solid catalyst with low crystal symmetry and a unique atomic arrangement can epitaxially grow a SWCNT with a designed chirality (**Figure 4a**).⁴ Tungsten-based intermetallic compounds with a rhombohedral structure were considered suitable candidates for this purpose. W tends to give the catalyst a high melting point and retain its crystalline structure during the CVD process while other components (Fe, Co, and Ni) provide the correct catalytic activity for SWCNT growth. *In situ* high-resolution (HR)TEM observations at 1100°C proved that W_6Co_7 nanoparticles maintained their crystal structure.⁷ In addition to a high melting point, the crystalline symmetry of the rhombohedral W_6Co_7 was low, both of which help the catalyst offer a structure to specifically recognize SWCNTs with different chiralities. Density

functional theory (DFT) simulations indicated that the (0 0 12) W_6Co_7 plane perfectly matches the (12, 6) tube (**Figure 4b**). With a W_6Co_7 catalyst prepared at 1030°C, (12, 6) tubes were obtained at an abundance of 92% (**Figure 4d**).⁷ HRTEM images of the SWCNT–catalyst interfaces showed that the (12, 6) tubes were always perpendicular to the (0 0 12) plane of the W_6Co_7 catalyst (**Figure 4c**).⁴ Furthermore, DFT simulations also revealed that (16, 0) tubes and (14, 4) tubes match the atomic arrangements of (1 1 6) plane and (1 0 10) plane of W_6Co_7 , respectively, (**Figure 4b**).^{26,27} The dominant growth of (16, 0) and (14, 4) tubes with the purity of 79% and 97%, respectively, were therefore realized at an optimized growth conditions (**Figure 4d**).^{26,27} A high melting point, low crystalline symmetry, and suitable catalytic activity are indispensable for catalysts designed to give chirality-selective growth of SWCNTs. Maruyama's group also realized the selective synthesis of (12, 6) with an enrichment of 50–70% using sputtered Co–W as the catalyst.⁴¹

Other than the atomic-level structural match, Zhang's group proposed a symmetry matching model based on the experimental results shown in **Figure 5a**.⁶ The edge of the SWCNTs and plane of the catalyst share a similar symmetry in thermodynamics, which was also proved by theoretical calculations (**Figure 5b**). They further optimized the kinetic growth conditions after considering the growth rate for different carbon nanotubes. Eventually, they obtained a sixfold symmetry (12, 6) nanotube array using sixfold Mo_2C catalysts and fourfold symmetry (8, 4) nanotubes from fourfold (1 0 0) WC catalysts, as shown in **Figure 5c**.⁶



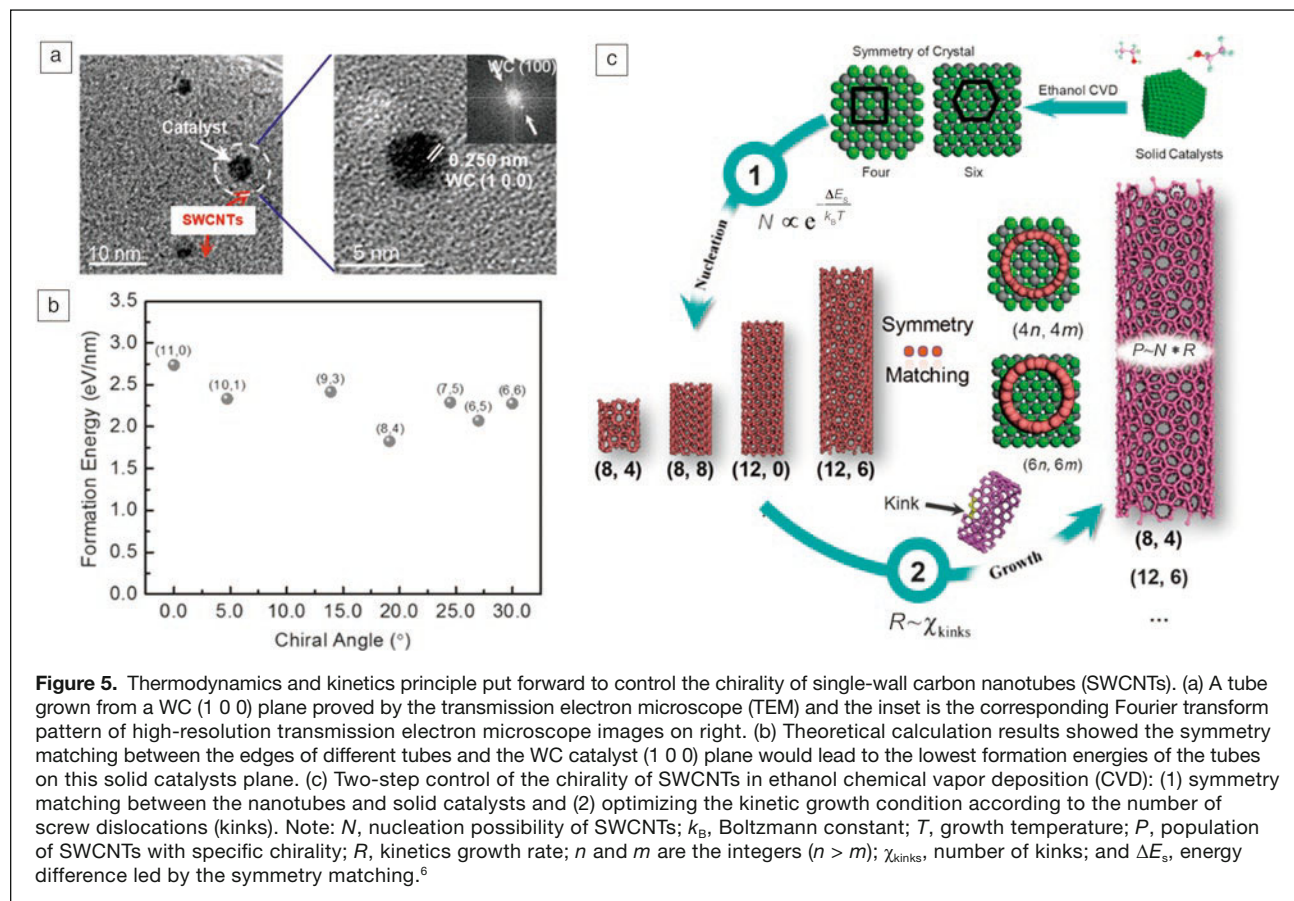


Figure 5. Thermodynamics and kinetics principle put forward to control the chirality of single-wall carbon nanotubes (SWCNTs). (a) A tube grown from a WC (1 0 0) plane proved by the transmission electron microscope (TEM) and the inset is the corresponding Fourier transform pattern of high-resolution transmission electron microscope images on right. (b) Theoretical calculation results showed the symmetry matching between the edges of different tubes and the WC catalyst (1 0 0) plane would lead to the lowest formation energies of the tubes on this solid catalysts plane. (c) Two-step control of the chirality of SWCNTs in ethanol chemical vapor deposition (CVD): (1) symmetry matching between the nanotubes and solid catalysts and (2) optimizing the kinetic growth condition according to the number of screw dislocations (kinks). Note: N , nucleation possibility of SWCNTs; k_B , Boltzmann constant; T , growth temperature; P , population of SWCNTs with specific chirality; R , kinetics growth rate; n and m are the integers ($n > m$); χ_{kinks} , number of kinks; and ΔE_s , energy difference led by the symmetry matching.⁶

Chirality-controlled growth of SWCNTs by supported catalysts on porous substrates

In the heterogeneous catalyst industry, catalysts are commonly loaded onto a porous substrate because the substrate has a large specific surface area that can load more catalyst, thus improving the yield of SWCNTs. Furthermore, the interactions between metal catalysts and porous substrates are usually stronger than those with a flat substrate. This strong interaction allows the catalysts to avoid sintering and keep their uniformity.

Porous or mesoporous SiO_2 , porous MgO , and zeolite are commonly used porous substrates for the growth of SWCNTs.⁴² It is obvious that the selection of the substrate will directly influence the formation of the catalyst and thus affect the growth of SWCNTs. Kauppinen et al. used SiO_2 -supported Co as the catalyst and realized the selective growth of (6, 5) SWCNTs.⁴³ The interaction between cobalt and the substrate facilitated the formation of uniform subnanometer Co catalysts, which favored the formation of small diameter SWCNTs.⁴⁴ Porous MgO was also used as the substrate for Co catalyst. FCC Co nanoparticles formed in CO through lattice-mismatched epitaxy from the $\text{Co}_x\text{Mg}_{1-x}\text{O}$ solid solution. Meanwhile, due to strong interaction between Co^{2+} and MgO in the solid solution, only Co^{2+} in the first few top atomic layers was reduced, thus forming uniform,

small-sized Co nanoparticles, which contributed to the preferential growth of (6, 5) with 53% purity.⁴⁵

In addition to the substrate, researchers also controlled the size and structure of the catalyst by introducing other metallic components to achieve chiral selective growth. Resasco et al. obtained (6, 5) SWCNTs with a purity of 54% using SiO_2 -supported CoMo catalysts.⁴⁶ The interactions between Mo oxides and Co stabilized the Co catalyst against aggregation, so the size of Co nanoparticles was small and uniform, which contributed to the preferential growth of (6, 5).⁴⁷ Similar results were also obtained for FeCu,^{48,49} CoMn,⁵⁰ CoCr,⁵¹ FeMn,⁵² and CoPt⁵³ catalysts. The involvement of uniform intermediates is an additional strategy to obtain catalyst nanoparticles with a narrow size distribution for chirality-selective growth of SWCNTs.^{54,55}

Catalysts for the bulk synthesis of SWCNTs: Synthesis, dispersion, and evaluation of the catalysts

Supported catalyst and free catalyst

Both supported and free catalysts have been used in synthesizing bulk CNTs. Catalysts can be preloaded onto a porous or flat substrate to grow CNTs. It has been reported that aligned CNTs can be synthesized in zeolite⁵⁶ or gel⁵⁷ templates with catalysts well dispersed in the nanopores. For the growth of

SWCNTs on flat substrates, catalyst nanoparticles or catalyst precursors are deposited on the substrates by solution routes^{9,58,59} or sputtering. The supported catalysts often offer precise control of the size, composition, and morphology of the particles.

A free catalyst features simultaneous formation of catalyst particles and the carbon feed source, which is more suitable for the continuous and bulk synthesis of CNTs. Wei's group have used this method in a designed nano-agglomerate fluidized-bed reactor, achieving bulk synthesis of aligned CNTs with a yield of 3 kg/h.⁶⁰ The product is now commercially available at CNano Technology Limited (China), however, a notable disadvantage is the difficulty in controlling the CNT diameter. Ago et al. proposed a method to narrow the diameter distribution by lowering the Fe loading on Fe/MgO catalysts⁶¹ (Figure 6a–b). This was attributed to the smaller catalyst particles formed when the metal loading amount was low, and the dominating surface diffusion on the catalyst particles resulted in the selective formation of SWCNTs.⁶² Despite that, further research is needed to precisely control the size and dispersion of catalyst particles for the stable bulk synthesis of CNTs.

Catalyst lifetime

The lifetime is a key characteristic among catalyst properties, especially for growing long CNTs. The lifetime of the catalyst is highly dependent on the reaction conditions. Liu's group developed a method to introduce marks on CNTs by reducing the carbon source concentration at designed times,⁶³ which can be post-identified and facilitate subsequent study of the kinetics (Figure 6c–d). Another approach involves an isotope labeling technique,⁶⁴ where ¹²C and ¹³C ethylene gases were fed into the reactor to reveal the growth mechanism and the growth rate.

Effects of support materials on the catalysts and bulk SWCNT growth

Conventional support materials and interactions with catalysts

The commonly used support materials in CVD include SiO₂, Al₂O₃, MgO, CaO, ZrO₂, TiO₂, and graphite. The choice of support material and catalyst determines the quality and yield of the as-grown SWCNTs, as shown by the following relationships: (1) Only certain combinations of catalyst and

substrate contribute significantly to SWCNT growth, such as Fe on Al₂O₃ or SiO₂, Co on MgO or Al₂O₃, and Ni-Co on silica;⁶⁵ (2) Inappropriate combinations of catalyst–and substrate decrease the catalytic activity; and (3) the catalyst–substrate interaction strongly affects the melting temperature of catalyst particles and thus the growth of SWCNTs. These catalyst–substrate relationships are attributed to their physical and chemical interactions. Physical interactions induced by van der Waals and electrostatic forces reduce the mobility of catalyst particles. For example, the theoretical study shows that supported catalysts possess higher melting temperatures than the free catalysts owing to reduced surface curvature in the former.⁶⁶

Meanwhile, there may be chemical interactions involving charge transfer and even reactions between catalysts and some substrates. Some supports such as oxide substrates are beneficial for not only SWCNT growth, but also the ultrafast growth of single-crystal graphene.⁶⁷ The researchers assume that the gradual release of oxygen from the substrates may significantly lower the energy barrier for the decomposition of carbon precursors.

Functional nanocomposites derived from CNTs and support materials

Some substrates such as alumina strongly interact with catalyst particles, allowing better metal dispersion and high-density SWCNT growth.⁸

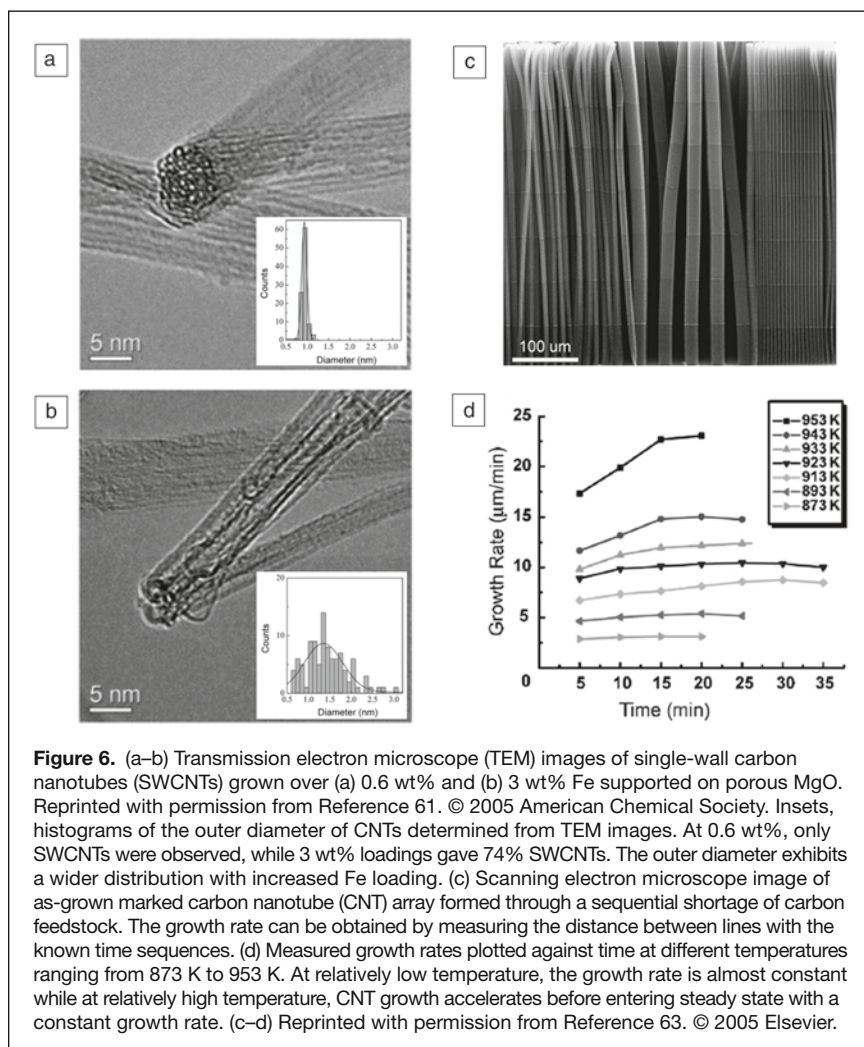
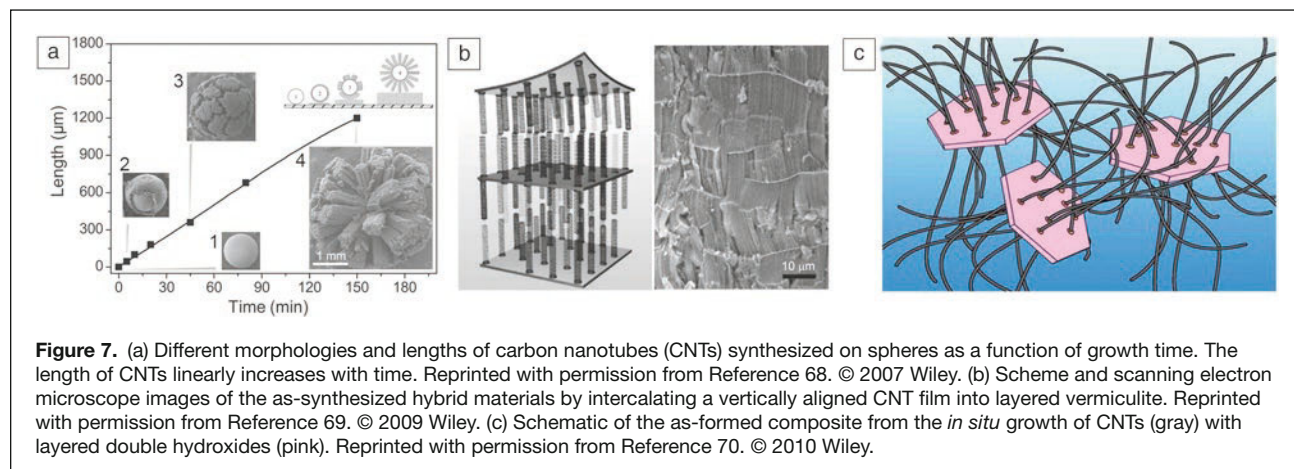


Figure 6. (a–b) Transmission electron microscope (TEM) images of single-wall carbon nanotubes (SWCNTs) grown over (a) 0.6 wt% and (b) 3 wt% Fe supported on porous MgO. Reprinted with permission from Reference 61. © 2005 American Chemical Society. Insets, histograms of the outer diameter of CNTs determined from TEM images. At 0.6 wt%, only SWCNTs were observed, while 3 wt% loadings gave 74% SWCNTs. The outer diameter exhibits a wider distribution with increased Fe loading. (c) Scanning electron microscope image of as-grown marked carbon nanotube (CNT) array formed through a sequential shortage of carbon feedstock. The growth rate can be obtained by measuring the distance between lines with the known time sequences. (d) Measured growth rates plotted against time at different temperatures ranging from 873 K to 953 K. At relatively low temperature, the growth rate is almost constant while at relatively high temperature, CNT growth accelerates before entering steady state with a constant growth rate. (c–d) Reprinted with permission from Reference 63. © 2005 Elsevier.



Although some substrates initially serve as a support for the as-grown CNTs, they may make substrate/CNT combination that can be utilized for subsequent applications. For example, Si/SiO₂ substrates are used for ultralong CNT growth, and the combination is suitable for use as gate electrodes for the direct fabrication of transistors.⁵⁸ Wei's group has developed a technique to make full use of natural support materials, not only as substrates, but also as functional hybrid materials. The initial strategy was related to the continuous production of aligned CNT arrays with millimeter-diameter spheres (Figure 7a) as substrates.⁶⁸ Layered vermiculite (a type of exfoliated clay compound) was further developed as a support (Figure 7b) for the production of CNT-based hybrid materials.⁶⁹ The introduction of strong yet flexible CNTs produced a highly ductile and resilient composite with an energy absorption capacity nearly 10× that of the original compounds.

Carbon-based nanocomposites supported by a layered double hydroxide, schematically shown in Figure 7c, exhibited excellent electrical conductivity, mechanical strength, and chemical reactivity.⁷⁰ These layered inorganic supports play vital roles in stabilizing the catalyst particles and preventing sintering at high temperature, and are also promising for applications in new generation functional composites.

Summary

Catalysts play critical roles in the growth of SWCNTs. The composition, size, and structure of the catalysts highly affect the structure and quality of the SWCNTs produced. In SWCNT growth on substrates, catalysts for the chirality-selective growth of SWCNTs with a high density are greatly needed. Catalysts with a high melting point, unique atomic arrangements, and reasonable activity are the rational choice for such a purpose. In the bulk synthesis of SWCNTs, future attention may shift from high-yield growth to structure-controlled growth. More efforts are needed in catalyst design for the bulk preparation of SWCNTs with specified structures.

References

1. A. Jorio, G. Dresselhaus, M.S. Dresselhaus, *Carbon Nanotubes: Advanced Topics in the Synthesis, Structure, Properties, and Applications* (Springer, Heidelberg, 2008).
2. Q. Zhang, J.-Q. Huang, W.-Z. Qian, Y.-Y. Zhang, F. Wei, *Small* **9**, 1237 (2013).
3. M. Kumar, Y. Ando, *J. Nanosci. Nanotechnol.* **10**, 3739 (2010).
4. F. Yang, X. Wang, M. Li, X. Liu, X. Zhao, D. Zhang, Y. Zhang, J. Yang, Y. Li, *Acc. Chem. Res.* **49**, 606 (2016).
5. J.R. Sanchez-Valencia, T. Dienel, O. Groning, I. Shorubalko, A. Mueller, M. Jansen, K. Amsharov, P. Ruffieux, R. Fasel, *Nature* **512**, 61 (2014).
6. S. Zhang, L. Kang, X. Wang, L. Tong, L. Yang, Z. Wang, K. Qi, S. Deng, Q. Li, X. Bai, *Nature* **543**, 234 (2017).
7. F. Yang, X. Wang, D. Zhang, J. Yang, D. Luo, Z. Xu, J. Wei, J.-Q. Wang, Z. Xu, F. Peng, X. Li, R. Li, Y. Li, M. Li, X. Bai, F. Ding, Y. Li, *Nature* **510**, 522 (2014).
8. Y. Hu, L. Kang, Q. Zhao, H. Zhong, S. Zhang, L. Yang, Z. Wang, J. Lin, Q. Li, Z. Zhang, *Nat. Commun.* **6**, 6099 (2015).
9. R. Zhang, Y. Zhang, Q. Zhang, H. Xie, W. Qian, F. Wei, *ACS Nano* **7**, 6156 (2013).
10. R. Zhang, Y. Zhang, F. Wei, *Acc. Chem. Res.* **50**, 179 (2017).
11. C. Liu, H.-M. Cheng, *J. Am. Chem. Soc.* **138**, 6690 (2016).
12. V.I. Artyukhov, E.S. Penev, B.I. Yakobson, *Nat. Commun.* **5**, 4892 (2014).
13. R. Saito, M. Fujita, G. Dresselhaus, M.S. Dresselhaus, *Appl. Phys. Lett.* **60**, 2204 (1992).
14. J. Li, K. Liu, S. Liang, W. Zhou, M. Pierce, F. Wang, L. Peng, J. Liu, *ACS Nano* **8**, 554 (2013).
15. Y. Yao, X. Dai, R. Liu, J. Zhang, Z. Liu, *J. Phys. Chem. C* **113**, 13051 (2009).
16. G. Zhang, D. Mann, L. Zhang, A. Javey, Y. Li, E. Yenilmez, Q. Wang, J.P. McVittie, Y. Nishi, J. Gibbons, *Proc. Natl. Acad. Sci. U.S.A.* **102**, 16141 (2005).
17. H. Dai, A.G. Rinzler, P. Nikolaev, A. Thess, D.T. Colbert, R.E. Smalley, *Chem. Phys. Lett.* **260**, 471 (1996).
18. C.L. Cheung, A. Kurtz, H. Park, C.M. Lieber, *J. Phys. Chem. B*, **106**, 2429 (2002).
19. P.E. Anderson, N.M. Rodriguez, *Chem. Mater.* **12**, 823 (2000).
20. C.L. Cheung, J.H. Hafner, C.M. Lieber, *Proc. Natl. Acad. Sci. U.S.A.* **97**, 3809 (2000).
21. Y. Li, J. Liu, Y. Wang, Z.L. Wang, *Chem. Mater.* **13**, 1008 (2001).
22. Y. Li, W. Kim, Y. Zhang, M. Rolandi, D. Wang, H. Dai, *J. Phys. Chem. B* **105**, 11424 (2001).
23. P. Yin, D. Li, T. Liu, *Chem. Soc. Rev.* **41**, 7368 (2012).
24. F. Peng, D. Luo, H. Sun, J. Wang, F. Yang, R. Li, J. Yang, Y. Li, *Chin. Sci. Bull.* **58**, 433 (2013).
25. S. Zhang, L. Tong, Y. Hu, L. Kang, J. Zhang, *J. Am. Chem. Soc.* **137**, 8904 (2015).
26. F. Yang, X. Wang, D. Zhang, K. Qi, J. Yang, Z. Xu, M. Li, X. Zhao, X. Bai, Y. Li, *J. Am. Chem. Soc.* **137**, 8688 (2015).
27. F. Yang, X. Wang, J. Si, X. Zhao, K. Qi, C. Jin, Z. Zhang, M. Li, D. Zhang, J. Yang, Z. Zhang, Z. Xu, L.-M. Peng, X. Bai, Y. Li, *ACS Nano* **11**, 186 (2016).
28. J. Chen, X. Xu, L. Zhang, S. Huang, *Nano-Micro Lett.* **7**, 353 (2015).
29. Y. Chen, J. Zhang, *Carbon* **49**, 3316 (2011).
30. H. Ago, T. Ayagaki, Y. Ogawa, M. Tsuji, *J. Phys. Chem. C* **115**, 13247 (2011).
31. Y. Yomogida, T. Tanaka, M. Zhang, M. Yudasaka, X. Wei, H. Kataura, *Nat. Commun.* **7**, 12056 (2016).
32. R.M. Jain, R. Howden, K. Tvrđy, S. Shimizu, A.J. Hilmer, T.P. McNicholas, K.K. Gleason, M.S. Strano, *Adv. Mater.* **24**, 4436 (2012).

33. C.M. Isborn, C. Tang, A. Martini, E.R. Johnson, A. Otero-de-la-Roza, V.C. Tung, *J. Phys. Chem. Lett.* **4**, 2914 (2013).
34. N. Murakami, Y. Tango, H. Miyake, T. Tajima, Y. Nishina, W. Kurashige, Y. Negishi, Y. Takaguchi, *Sci. Rep.* **7**, 43445 (2017).
35. F. Zhang, P.-X. Hou, C. Liu, H.-M. Cheng, *Carbon* **102**, 181 (2016).
36. M. Li, X. Liu, X. Zhao, F. Yang, X. Wang, Y. Li, *Top. Curr. Chem.* **375**, 29 (2017).
37. Y. Wang, M.J. Kim, H. Shan, C. Kittrell, H. Fan, L.M. Ericson, W.-F. Hwang, S. Arepalli, R.H. Hauge, R.E. Smalley, *Nano Lett.* **5**, 997 (2005).
38. S. Reich, L. Li, J. Robertson, *Chem. Phys. Lett.* **421**, 469 (2006).
39. M. Fouquet, B. Bayer, S. Esconjauregui, R. Blume, J. Warner, S. Hofmann, R. Schlögl, C. Thomsen, J. Robertson, *Phys. Rev. B* **85**, 235411 (2012).
40. N. Ishigami, H. Ago, K. Imamoto, M. Tsuji, K. Iakoubovskii, N. Minami, *J. Am. Chem. Soc.* **130**, 9918 (2008).
41. H. An, A. Kumamoto, H. Takezaki, S. Ohyama, Y. Qian, T. Inoue, Y. Ikuhara, S. Chiashi, R. Xiang, S. Maruyama, *Nanoscale* **8**, 14523 (2016).
42. H. Wang, Y. Yuan, L. Wei, K. Goh, D.S. Yu, Y. Chen, *Carbon* **81**, 1 (2015).
43. M. He, A.I. Chernov, P.V. Fedotov, E.D. Obraztsova, E. Rikkinen, Z. Zhu, J. Sainio, H. Jiang, A.G. Nasibulin, E.I. Kauppinen, M. Niemelä, A.O.I. Krause, *Chem. Commun.* **47**, 1219 (2011).
44. N. Li, X. Wang, S. Derrouiche, G.L. Haller, L.D. Pfefferle, *ACS Nano* **4**, 1759 (2010).
45. M. He, H. Jiang, B. Liu, P.V. Fedotov, A.I. Chernov, E.D. Obraztsova, F. Cavalca, J.B. Wagner, T.W. Hansen, I.V. Anoshkin, E.A. Obraztsova, A.V. Belkin, E. Sairanen, A.G. Nasibulin, J. Lehtonen, E.I. Kauppinen, *Sci. Rep.* **3**, 1460 (2013).
46. G. Loll, L. Zhang, L. Balzano, N. Sakulchaicharoen, Y. Tan, D.E. Resasco, *J. Phys. Chem. B* **110**, 2108 (2006).
47. S.M. Bachilo, L. Balzano, J.E. Herrera, F. Pompeo, D.E. Resasco, R.B. Weisman, *J. Am. Chem. Soc.* **125**, 11186 (2003).
48. M. He, A.I. Chernov, P.V. Fedotov, E.D. Obraztsova, J. Sainio, E. Rikkinen, H. Jiang, Z. Zhu, Y. Tian, E.I. Kauppinen, *J. Am. Chem. Soc.* **132**, 13994 (2010).
49. M. He, B. Liu, A.I. Chernov, E.D. Obraztsova, I. Kauppi, H. Jiang, I. Anoshkin, F. Cavalca, T.W. Hansen, J.B. Wagner, A.G. Nasibulin, E.I. Kauppinen, J. Linnekoski, M. Niemelä, J. Lehtonen, *Chem. Mater.* **24**, 1796 (2012).
50. C.Z. Loebick, S. Derrouiche, N. Marinkovic, C. Wang, F. Hennrich, M.M. Kappes, G.L. Haller, L.D. Pfefferle, *J. Phys. Chem. C* **113**, 21611 (2009).
51. C. Zoican Loebick, S. Derrouiche, F. Fang, N. Li, G.L. Haller, L.D. Pfefferle, *Appl. Catal. A Gen.* **368**, 40 (2009).
52. M. He, P.V. Fedotov, A. Chernov, E.D. Obraztsova, H. Jiang, N. Wei, H. Cui, J. Sainio, W. Zhang, H. Jin, M. Karppinen, E.I. Kauppinen, A. Loiseau, *Carbon* **108**, 521 (2016).
53. B. Liu, W. Ren, S. Li, C. Liu, H.-M. Cheng, *Chem. Commun.* **48**, 2409 (2012).
54. H. Wang, B. Wang, X.Y. Quek, L. Wei, J. Zhao, L.J. Li, M.B. Chan-Park, Y. Yang, Y. Chen, *J. Am. Chem. Soc.* **132**, 16747 (2010).
55. Y. Yuan, H.E. Karahan, C. Yildirim, L. Wei, Ö. Birer, S. Zhai, R. Lau, Y. Chen, *Nanoscale* **8**, 17705 (2016).
56. M. Kumar, Y. Ando, *Carbon* **43**, 533 (2005).
57. W.Z. Li, S.S. Xie, L.X. Qian, B.H. Chang, B.S. Zou, W.Y. Zhou, R.A. Zhao, G. Wang, *Science* **274**, 1701 (1996).
58. Z. Zhu, N. Wei, H. Xie, R. Zhang, Y. Bai, Q. Wang, C. Zhang, S. Wang, L. Peng, L. Dai, F. Wei, *Sci. Adv.* **2**, e1601572 (2016).
59. X. Wang, Q. Li, J. Xie, Z. Jin, J. Wang, Y. Li, K. Jiang, S. Fan, *Nano Lett.* **9**, 3137 (2009).
60. Q. Zhang, M.-Q. Zhao, J.-Q. Huang, J.-Q. Nie, F. Wei, *Carbon* **48**, 1196 (2010).
61. H. Ago, S. Imamura, T. Okazaki, T. Saito, M. Yumura, M. Tsuji, *J. Phys. Chem. B* **109**, 10035 (2005).
62. Q. Zhang, J.-Q. Huang, M.-Q. Zhao, W.-Z. Qian, F. Wei, *ChemSusChem* **4**, 864 (2011).
63. K. Liu, K. Jiang, C. Feng, Z. Chen, S. Fan, *Carbon* **43**, 2850 (2005).
64. L. Liu, S. Fan, *J. Am. Chem. Soc.* **123**, 11502 (2001).
65. A.R. Harutyunyan, *J. Nanosci. Nanotechnol.* **9**, 2480 (2009).
66. A. Jiang, N. Awasthi, A.N. Kolmogorov, W. Setyawan, A. Börjesson, K. Bolton, A.R. Harutyunyan, S. Curtarolo, *Phys. Rev. B Condens. Matter* **75**, 205426 (2007).
67. X. Xu, Z. Zhang, L. Qiu, J. Zhuang, L. Zhang, H. Wang, C. Liao, H. Song, R. Qiao, P. Gao, Z. Hu, L. Liao, Z. Liao, D. Yu, E. Wang, F. Ding, H. Peng, K. Liu, *Nat. Nanotechnol.* **11**, 930 (2016).
68. R. Xiang, G.H. Luo, W.Z. Qian, Y. Wang, F. Wei, Q. Li, *Chem. Vapor Depos.* **13**, 533 (2007).
69. Q. Zhang, M. Zhao, Y. Liu, A. Cao, W. Qian, Y. Lu, F. Wei, *Adv. Mater.* **21**, 2876 (2009).
70. M.-Q. Zhao, Q. Zhang, X.-L. Jia, J.-Q. Huang, Y.-H. Zhang, F. Wei, *Adv. Funct. Mater.* **20**, 677 (2010). □



Xiulan Zhao is a doctoral candidate in the College of Chemistry and Molecular Engineering at Peking University, China. She earned her bachelor's degree in chemistry from Shandong University, China, in 2013. Her research interests mainly focus on chirality-controlled synthesis of single-wall carbon nanotubes. Zhao can be reached by phone at +86-10-62754167 or by email at xiulanzhls@pku.edu.cn.



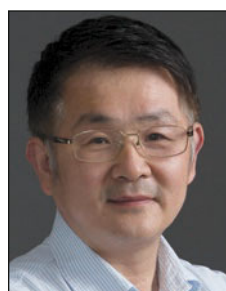
Shuchen Zhang is a postdoctoral researcher at Peking University, China. He received his BS degree from Shandong University, China, in 2012, and his PhD degree at Peking University. His research interests mainly focus on the preparation and properties of low-dimensional nanomaterials, including the structure-controlled growth of single-wall carbon nanotubes and their related applications. Zhang can be reached by phone at +86-10-62757157 or by email at zhangsc-cnc@pku.edu.cn.



Zhenxing Zhu is a doctoral candidate in the Department of Chemical Engineering at Tsinghua University, China. He obtained his bachelor's degree in the Department of Chemical Engineering and Technology from Beijing University of Chemical Technology, China, in 2015. His research interests focus on the controlled synthesis, characterization, and growth mechanism of ultralong carbon nanotubes. Zhu can be reached by phone at +86 13301390972 or by email at zzx15@mails.tsinghua.edu.cn.



Jin Zhang was appointed as Changjiang Professor at Peking University, China, in 2013. He received his PhD degree from Lanzhou University, China, in 1997. After a postdoctoral fellowship at the University of Leeds, UK, he returned to Peking University, where he was appointed associate professor in 2000 and promoted to full professor in 2006. He is a Fellow of the Royal Society of Chemistry. His research focuses on the controlled synthesis and spectroscopic characterization of carbon nanomaterials. He has published more than 220 articles. Zhang can be reached by email at jinzhang@pku.edu.cn.




Fei Wei is a professor of chemical engineering at Tsinghua University, China. He obtained his PhD degree in chemical engineering from China University of Petroleum in 1990. After a postdoctoral fellowship at Tsinghua University, he was appointed associate professor in 1992 prior to being appointed professor in 1996. He has also been a visiting professor at The Ohio State University, University of Western Ontario, Canada, and Nagoya Institute of Science and Technology, Japan. His research interests include chemical-reaction engineering, multiphase flow, advanced materials, and sustainable energy. Wei can be reached by email at wf-dce@mail.tsinghua.edu.cn.



Yan Li has been full professor of chemistry at Peking University, China, since 2002. She received her PhD degree in inorganic chemistry from Peking University in 1993. From 1999 to 2001, she was a visiting associate professor at Duke University. She was designated a Chang Jiang Scholar by the Chinese Ministry of Education in 2014. She has held a distinguished visiting professorship at The University of Tokyo, Japan, since 2016. She is a Fellow of the Royal Society of Chemistry. She serves as associate editor for the journal *ACS Nano* and is on the advisory boards of the journals *Materials Horizons* and *Journal of Materials Chemistry A*.

Her research focuses on the preparation, modification, characterization, and application of carbon nanotubes. Li can be reached by phone at +86-10-62756773 or by email at yanli@pku.edu.cn.

CALL FOR PAPERS



Journal of MATERIALS RESEARCH



July 2018
3D Printing of Biomaterials
Submission Deadline—
February 1, 2018

www.mrs.org/jmr

JANIS

Cryogenic Products for Nanotechnology



MRS Booth 410

Janis has long been the first stop for cryogenic tools for materials characterization, but we can also help with nanoscale applications.

Contact Janis to talk with an applications engineer. We can help you find the right cryostat for your application.

Typical applications include:

- UV-Vis-IR optical measurements
- Microscopy
- High Tc superconductors
- Nanoscale electronics
- High frequency measurements
- Spintronics
- Terahertz detectors and devices
- Photovoltaics
- Non-destructive device and wafer testing

Contact us today: sales@janis.com
www.janis.com/Nanotechnology.aspx
www.facebook.com/JanisResearch

INTERNATIONAL CENTRE FOR DIFFRACTION DATA

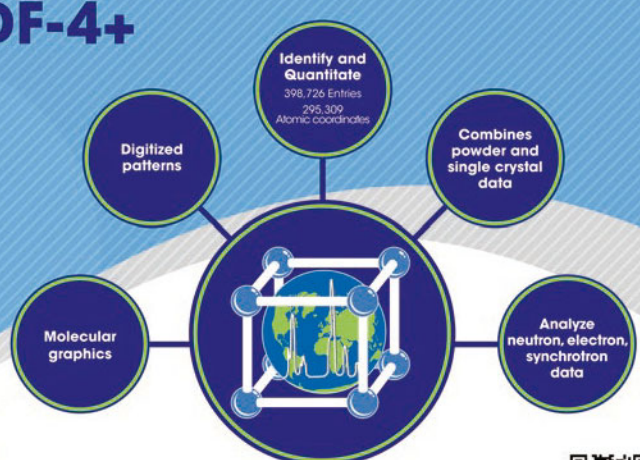
Diffraction Data You Can Trust


ICDD databases are the only crystallographic databases in the world with quality marks and quality review processes that are ISO certified.

PDF-4+


- Standardized Data
- More Coverage
- All Data Sets Evaluated For Quality
- Reviewed, Edited and Corrected Prior To Publication
- Targeted For Material Identification and Characterization



Visit us at MRS Booth 409





ICDD
INTERNATIONAL CENTRE FOR DIFFRACTION DATA



www.icdd.com | marketing@icdd.com

ICDD, the ICDD logo and PDF are registered in the U.S. Patent and Trademark Office. Powder Diffraction File is a trademark of JCPDS - International Centre for Diffraction Data ©2017 JCPDS-International Centre for Diffraction Data - 10/17